

Resonant-Cavity Light-Emitting Diodes*

E. F. Schubert, N. E. J. I-Hunt, D. L. Çivco and A. Y. Cho
AT&T Bell Laboratories, Murray Hill, New Jersey 07974

Received July 12, 1993; revised manuscript received September 17, 1993

Resonant-cavity light-emitting diodes (RCLEDs) are a new generation of LEDs which have an active region inside a planar Fabry-Perot micro-cavity. The cavity is resonant with the emission wavelength of the active region. RCLEDs exhibit directed emission of very high spectral purity and have enhanced efficiency as compared to conventional LEDs, which makes RCLEDs attractive for applications in silica fiber based communication systems.

Light-emitting diodes (LEDs) are widely used as sources in short and medium distance optical fiber communications because of their reliability, low cost, temperature insensitivity, and large fiber-alignment tolerances^[1]. There is considerable interest, therefore, in improving the efficiency and spectral characteristics of light-emitting diodes. The resonant-cavity light-emitting diode (RCLED) is a new type of LED with improved spectral purity as well as enhanced intensity^[2-4]. The RCLED has the active region (pn-junction) inside a Fabry-Pérot micro-cavity. One of the cavity modes (usually the fundamental mode) is in resonance with the emission wavelength of the active semiconductor. As a result of the micro-cavity, the emission characteristics of this device are changed dramatically.

The reflectors of the cavity can be either distributed Bragg reflectors (DBRs) or metallic reflectors (e.g. Au or Ag). The distributed Bragg reflectors consist of a stack of two alternating materials with different refractive indices. The thickness of each layer in the DBR is one quarter of the resonance wavelength of the cavity. Very high reflectivities can be obtained, if the two materials constituting the DBR are fully transparent at the wavelength of interest. Reflectivities > 99% have been reported using such DBRs^[5]. Metallic reflectors, in particular silver (Ag), have reflectivities of 98-99% at the air-Ag interface and 95-97% for the GaAs-Ag interface^[6]. The magnitude of the GaAs-Ag reflectivity is sufficiently high for RCLED applications.

In order to illustrate the principle of the RCLED we first consider a planar Fabry-Pérot cavity illustrated in Fig. 1. The cavity consists of two co-planar reflectors

with reflectivities R_1 and R_2 . The phase shift incurred by the electromagnetic wave upon reflection is assumed to be $\phi_1 = \phi_2 = 0$. Planar waves propagating along the optical axis of the cavity can either constructively or destructively interfere with themselves, as shown in Fig. 1. Whereas constructively interfering waves can form stationary modes in the cavity, destructively interfering modes annihilate themselves and therefore cannot exist in a cavity. The optical modes are referred to as allowed modes and disallowed modes, respectively.

Assuming perfect reflectors of the cavity with $R = R_1 = R_2 = 1$ and no absorption losses inside the cavity, photons cannot escape from the cavity. In such an ideal cavity, the spectrum of allowed modes is a train of δ -functions^[7], as illustrated in Fig. 1. The mode of lowest frequency, ν_0 , is the fundamental cavity mode. For $\phi = \phi_1 = \phi_2 = 0$, the wavelength of the fundamental mode is given by $\lambda = 2L_c$, where L_c is the cavity length.

Whereas the photon lifetime in an ideal cavity is infinite, the photon lifetime in any real cavity is finite. The finiteness of the lifetime can be due to either non-perfect reflectors, i.e. $R_1 < 1$ and $R_2 < 1$ or due to absorption losses inside the cavity. As a consequence, the cavity modes are spectrally broadened, as illustrated in Fig. 1. The broadening can be deduced from the uncertainty relation $\Delta E \tau \cong h$, where $\Delta E = h \Delta \nu$ is the broadening of the optical mode, τ is the photon lifetime inside the cavity, and h is Planck's constant. Assuming a transparent cavity medium (no absorption) and the reflectivities R_1 and R_2 , the average cavity escape probability per single pass of a photon inside the cavity is given by

*Invited talk.

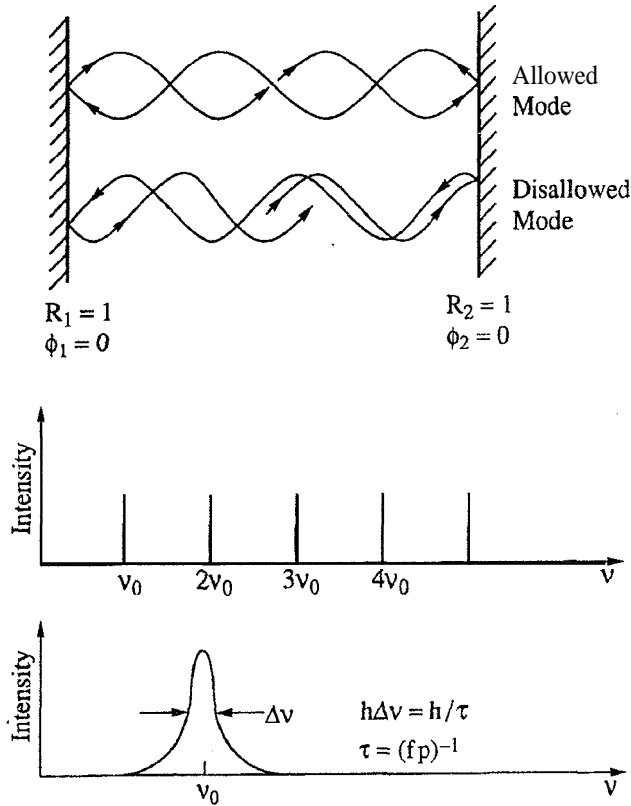


Figure 1: Optical resonator consisting of two reflectors with reflectivities R_1 and R_2 and phase shifts ϕ_1 and ϕ_2 . The spectrum of allowed modes of an ideal cavity ($R = R_1 = R_2 = 1$) consists of train of δ -functions. For a cavity with $R < 1$, the allowed modes are broadened. The mode broadened $\Delta\nu$ can be calculated from the uncertainty relation $\Delta E \Delta \tau \leq h$.

where we assumed $R_1 \cong R_2 \cong 1$. The mean photon lifetime inside the cavity is then given by

$$\tau = (fp)^{-1} = \frac{nL_c}{c} \frac{1}{1 - \sqrt{R_1 R_2}} \quad (2)$$

where $f = c/nL_c$ is the oscillation frequency of the photon inside the cavity: n is the refractive index of the cavity medium, and L , is the cavity length. Using Eqs. (1) and (2), the broadening of the modes is given by

$$\begin{aligned} Q &= \frac{E}{\Delta E} = \frac{\nu}{\Delta \nu} = \frac{\lambda}{\Delta \lambda} \\ &= 2\pi \frac{L_c}{\lambda} \frac{1}{1 - \sqrt{R_1 R_2}} \end{aligned} \quad (3)$$

where Q is called the cavity quality factor.

We next consider an optically active medium, for example a semiconductor, inside a planar cavity. At room temperature, the semiconductor has a natural emission spectrum that reflects the thermal distribution of elec-

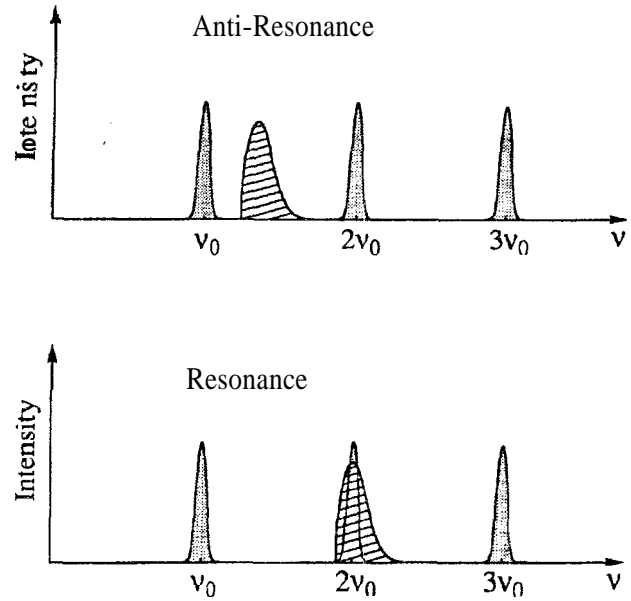


Figure 2: Schematic natural emission spectrum and broadened optical modes of a resonator. The natural emission spectrum does and does not overlap with a resonator mode for the resonance and off-resonance cavity, respectively.

trons and holes in the bands. The theoretical spectral width of the band-to-band transition is $1.8 kT$ [8] which can be much broader than the broadened optical mode of the cavity. The natural emission spectrum of the semiconductor can be either in resonance or off-resonance with one of the cavity modes, as schematically illustrated in Fig. 2. We first consider the case of off-resonance and discuss the spontaneous emission of photons along the optical axis of the cavity. As illustrated in Fig. 2, no overlap exists between the mode distribution and the natural emission spectrum. Therefore, photon emission along the optical axis of the cavity is inhibited for any non-resonant wavelength. That is, the emission probability is low for off-resonance emission and the corresponding lifetime is long.

We next consider a cavity which has an optical mode in resonance with the natural emission spectrum of the semiconductor. We assume that the cavity mode is narrower than the natural emission spectrum of the semiconductor, as illustrated in Fig. 2. As a first consequence of the cavity, the optical emission of the structure has a narrower linewidth, i.e. a higher spectral purity as compared to the natural emission spectrum of the semiconductor. That is, the lineshape of the emission is determined by the shape of the cavity mode rather than by the thermal distribution of carriers in the

bands of the semiconductor. Very pure spectral emission with linewidths $\ll kT$ have indeed been observed in RCLEDs^{2-4]}.

As a second consequence of the cavity, the on-resonance emission of the semiconductor is drastically enhanced. The enhancement factor G_e has been determined to be^[4]

$$G_e = \frac{(1 + \sqrt{R_2})^2(1 - R_1)}{(1 - \sqrt{R_1 R_2})^2} \quad (4)$$

where R_1 is the reflectivity of the light-exit mirror, R_2 is the high-reflectivity back-side mirror, and $R_2 > R_1$ has been assumed. Equation (4) is valid if the optically active medium is at the anti-node position of the standing optical wave inside the cavity. For typical semiconductor structures, the emission enhancement G_e can assume values of 50-100 at the resonance wavelength^[4]. Knowing the emission spectrum of the active medium without cavity, Eqs. (3) and (4) allow one to determine the enhancement of integrated intensity compared to a structure without mirrors. We estimate the integrated intensity enhancement to be a factor of 8 in the structure described in this publication.

The structure and layer sequence of an RCLED is shown in Fig. 3. The sequence of epitaxial layers of the structure, which was grown by molecular-beam epitaxy, consists of an n^+ -type GaAs substrate, a 12 period DBR., an AlGaAs confinement layer, 4 strained GaInAs quantum wells with GaAs barriers, a second AlGaAs confinement layer, and a p^+ -type GaAs contact layer. The top Ag electrode serves as a top reflector as well as an ohmic contact to the semiconductor. The top contact has a diameter of 20 μm and is defined by SiO_2 . Ti/Au metallization is used as bonding pad for the diode. AuGe metallization alloyed at 400°C for 20 seconds forms the back-side contact. Light emission occurs through a window in the AuGe contact. The window is coated with cubic zirconium ($\text{ZrO}_2\text{:Y}$) which serves as an anti-reflection coating. We estimate the reflectivity of the top and bottom reflector to be 96% and 92% respectively.

The room-temperature emission spectrum of the RCLED is shown in Fig. 4. The RCLED spectrum exhibits a single line at 937 nm of high spectral purity. The full-width at half-maximum of the spectrum is only 5 nm corresponding to 7 meV. Note that the linewidth is much narrower than kT (25 meV) at room

temperature. The current used to drive the LED is 14 mA.

Figure 4 also shows the optical spectrum of a commercial GaAs LED (AT&T optical data link, ODL 50 Mbit/sec) at a drive current of 40 mA. This LED has the same contact diameter (20 μm) as the RCLED. The LED spectrum is 50 nm wide corresponding to 80 meV, i.e. approximately a factor of 10 wider than the RCLED spectrum. The narrow spectrum of the RCLED may allow it to be used in wavelength division multiplexing applications, where several signals are sent along the same fiber at slightly different wavelengths. The narrow RCLED spectrum is also beneficial for reducing the chromatic dispersion of a signal sent over several kilometers of optical fiber.

The optical power vs. current curve for the RCLED at 300K is shown in Fig. 5. Shown is the far field intensity in the normal direction on the right vertical axis, and the butt-coupled power into a 62.5 μm graded index multi-mode fiber on the left vertical axis. The far field and coupled power curves are the identical shape, and can be shown as a single curve. The output efficiency of the device is very high for currents less than 14 mA, but starts saturating at higher currents due to the effects of band filling. Even further optimization of the device efficiency should be possible. Butt-coupling to the substrate underfills the 0.29 numerical aperture of the fiber, so coupled power can always be increased by lensing. Further processing to create an integrated lens etched into the GaAs substrate would typically increase the coupling efficiency to the fiber by a factor of 2.5-3, while only slightly increasing the coupled spectral width.

We finally compare the RCLED structure with that of a vertical-cavity surface-emitting laser (VCSEL). We note that the two devices, although both devices have basically similar structures, have two significant differences. First, the mirror reflectivities of the RCLED are much lower than the reflectivities required in a VCSEL. In the laser structure, very high reflectivities, typically exceeding 99%, are required due to the short gain length

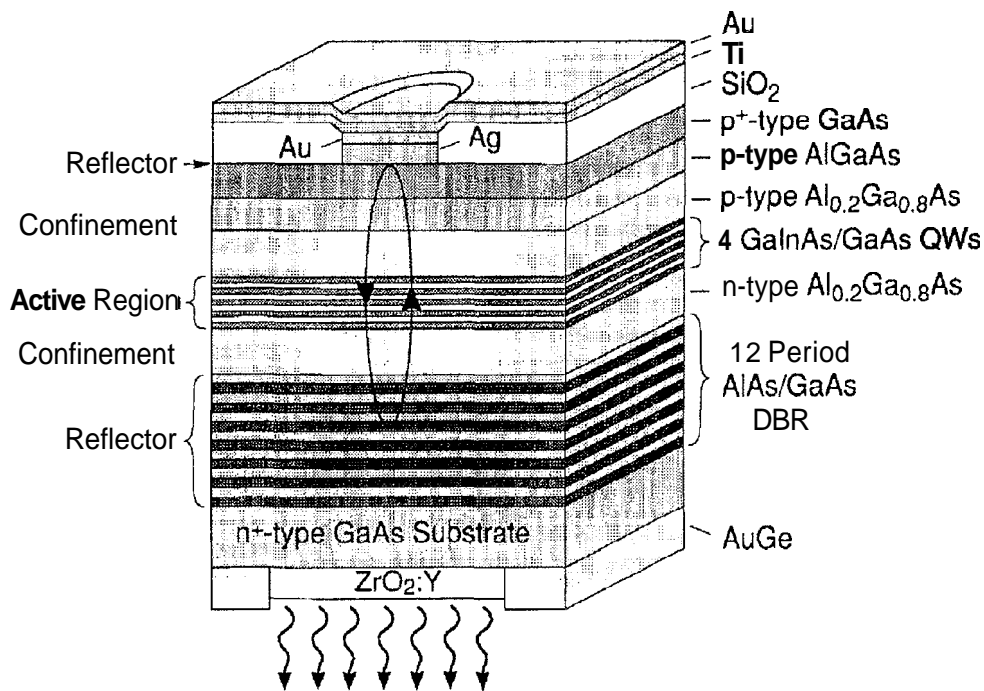


Figure 3: Schematic illustration of a GaAs/GaInAs/AlGaAs RCLED with one silver (Ag) mirror and one distributed Bragg reflector (DBR).

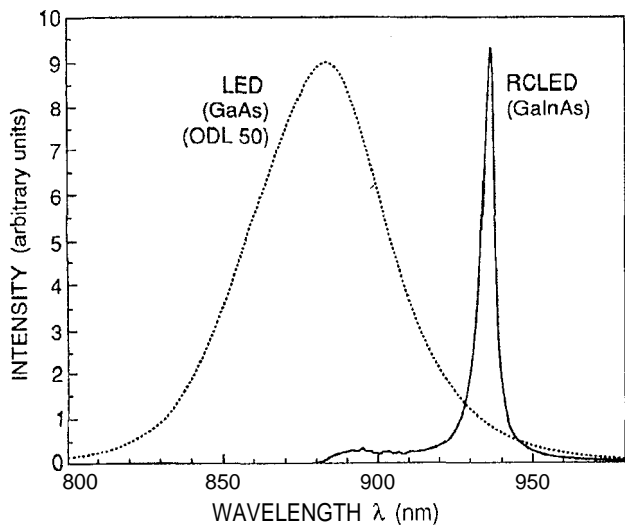


Figure 4: Optical emission spectra at $T = 300\text{K}$ of a conventional AlGaAs/GaAs LED (dashed line) and of a AlGaAs/GaAs/GaInAs RCLED (solid line).

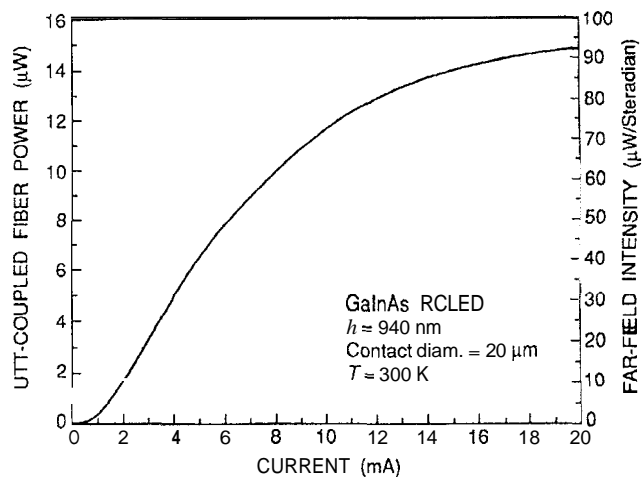


Figure 5: Light-intensity-versus-current curve of an RCLED. The left ordinate shows the power butt-coupled into a $62.5\ \mu\text{m}$ core graded-index multi-mode fiber. The right ordinate shows the far-field intensity in the normal direction.

of such lasers^[5]. For RCLEDs, the required reflectivities are much lower, typically 85-95% for the light-exit reflector and 95-99% for the back-side mirror. Fabrication and manufacturing requirements for RCLEDs will be therefore relaxed as compared to VCSELs. Second, in RCLEDs the re-absorption probability of photons in the active area, αL_{active} is much lower than the photon transmission probability through the exit reflector, $(1 - R_1)$. This condition ensures that, at all pump levels and operating temperatures, the self-absorption of the cavity does not appreciably quench the cavity resonance, and therefore the output power. This lack of self-absorption is generally not met by VCSELs^[5], which results in very small spontaneous emission intensities for VCSELs pumped below threshold^[4].

In summary, we have presented a novel concept for a light-emitting diode which consists of a pn-junction diode and a Fabry-Pérot micro-cavity. The fundamental optical mode of the cavity is in resonance with the emission wavelength of the active medium. The resonant-cavity light-emitting diode offers several attractive features such as a high spectral purity of the emission and an enhanced integrated intensity of the emission as compared to conventional LEDs. Experimental results demonstrate that linewidths of RCLEDs are ten times narrower than those of conventional LEDs. Chromatic dispersion is therefore reduced in RCLED-based communication systems. These features make the device attractive for short and medium distance optical communication systems and will allow for lower drive currents, higher bit rates, and longer transmission distances.

Acknowledgements

The authors gratefully acknowledge useful contributions and discussions with J. A. Lourenco, W. C. King, R. H. Saul, L.-W. Tu, R. A. Logan, and G. J. Zydzik.

References

1. R. H. Saul, T. I. Lee, and C. A. Burrus, in *Semiconductors and Semimetals*, (Academic, New York, 1985). Vol. 22, Part C, p. 193
2. E. F. Schubert, Y. H. Wang, A. Y. Cho, L.-W. Tu, and G. J. Zydzik, *Appl. Phys. Lett.* **60**, 921 (1992).
3. N. E. J. Hunt, E. F. Schubert, R. A. Logan, and G. J. Zydzik, *Appl. Phys. Lett.* **61**, 2287 (1992).
4. N. E. J. Hunt, E. I. Schubert, R. F. Kopf, D. L. Sivco, A. Y. Cho, and G. J. Zydzik, *Appl. Phys. Lett.* **63**, 2600 (1993).
5. J. L. Jewell, J. P. Harbison, A. Scherer, Y. H. Lee, and L. T. Florez, *IEEE J. Quantum Electron* **27**, 1332 (1991).
6. E. F. Schubert, L.-W. Tu, R. F. Kopf, G. J. Zydzik, and D. G. Deppe, *Appl. Phys. Lett.* **57**, 117 (1990).
7. M. Born and E. Wolf, *Principles of Optics* (Pergamon, Oxford, 1980).
8. E. F. Schubert, *Doping in III-V Semiconductors*, (Cambridge University Press, Cambridge, 1993) p. 520.